 DOI: 10.1002/masy.200850502

Broadband Dielectric Relaxation Spectroscopy in Polymer Nanocomposites

Polycarpos Pissis,[*1] *Daniel Fragiadakis,*[1] *Athanasios Kanapitsas,*[2] *Kostas Delides*[3]

Summary: Dielectric spectroscopy in the frequency domain and thermally stimulated depolarization currents techniques, covering together a broad frequency range (10^{-4} – 10^{9} Hz), were employed to investigate molecular dynamics in relation to structure and morphology in polymeric nanocomposites. Several systems were investigated, three of them with the same epoxy resin matrix and different inclusions (modified smectite clay, conducting carbon nanoparticles and diamond nanoparticles) and two with silica nanofiller (styrene-butadiene rubber/silica and polyimide/silica nanocomposites). Special attention was paid to the investigation of segmental dynamics associated with the glass transition of the polymer matrix, in combination also with differential scanning calorimetry measurements. Effects of nanoparticles on local (secondary) relaxations and on the overall dielectric behavior were, however, also investigated. Several interesting results were obtained and discussed for each of the particular systems. Two opposite effects seem to be common to the nanocomposites studied and dominate their behavior: (1) immobilization/reduction of mobility of a fraction of the chains at the interface to the inorganic nanoparticles, due to chemical or physical bonds with the particles, and (2) loosened molecular packing of the chains, due to tethering and geometrical confinement, resulting in an increase of free volume and of molecular mobility.

Keywords: dielectric spectroscopy; glass transition; polymer nanocomposites; segmental dynamics

Introduction

The mechanical and the physical properties of polymer nanocomposites, i.e. composite materials with a polymeric matrix and, typically, inorganic fillers with characteristic size in the range of 1–100 nm, are often significantly improved, as compared to those of the polymer matrix, for much smaller filler content than would be required for conventional macroscale or microscale composites.[1,2] Polymer nanocomposites also exhibit distinctive properties related to the small particle size and correspondingly small mean interparticle spacing (typically also in the nanometer range).[3]

There is yet no satisfactory theoretical explanation for the origin of improvement of the properties of polymer nanocomposites. It is generally accepted, however, that the large surface to volume ratio of the nanoscale inclusions plays a significant role. Results obtained by various experimental techniques, as well as by theory and computer simulations, indicate the presence of an interfacial polymer layer around the filler, with structure/morphology and chain dynamics modified with respect to the bulk polymer matrix.[4–9] The existence of such an interfacial layer has been postulated for conventional composites long ago and various experiments provided

[1] National Technical University of Athens, Department of Physics, Zografou Campus, 157 80 Athens, Greece
E-mail: ppissis@central.ntua.gr
[2] Technological Education Institute (TEI) of Lamia, Department of Electronics, 35100 Lamia, Greece
[3] Technological Education Institute (TEI) of West Macedonia, Laboratories of Physics and Materials Technology, Kozani, Greece

support for that.[10,11] Questions related to the existence of such an interfacial layer, its thickness and the variation of polymer properties within the layer with respect to bulk properties become crucial for nanocomposites. The reason for that is that, due to the small particle size, resulting in a large surface area presented to the polymer by the nanoparticles, the interfacial layer can represent a significant volume fraction of the polymer in nanocomposites.[3]

Broadband dielectric relaxation spectroscopy (DRS) has proved to be a powerful tool for investigation of molecular dynamics of polymers and composites.[12,13] The main advantage of DRS, as compared to other similar techniques for studying molecular dynamics, is the broad frequency range, which can be relatively easily covered[13] (10^{-4}–10^{9} Hz in the present work). This broad frequency range allows to measure on the same sample processes with very different characteristic (relaxation) times and, correspondingly, different characteristic length scales.

Guided by theory and by results obtained with model systems of geometrical confinement, we have investigated over the last few years molecular dynamics in nanostructured polymers and in polymer nanocomposites with various matrices and fillers. To that aim we employed ac dielectric spectroscopy in the frequency domain and, to a lesser extent, a second dielectric technique in the temperature domain, thermally stimulated depolarization currents – TSDC, differential scanning calorimetry (DSC) and dynamic mechanical analysis (DMA). Here we present and discuss comparatively to each other results obtained with five selected nanocomposite systems, three of them with the same epoxy resin matrix and different inclusions (modified smectite clay, conducting carbon nanoparticles and diamond nanoparticles) and two with silica nanofiller (styrene-butadiene rubber/silica and polyimide/silica nanocomposites). The preparation of the nanocomposites, the morphological characterization and details of the dynamics studies have been presented/will be presented for each particular system elsewhere. In this comparative study we focus on common features and differences in the effects of nanoparticles on the polymer matrix dynamics, as revealed by dielectric techniques. Effects on the overall dielectric behavior, on local (secondary) relaxations and, in particular, on segmental dynamics, associated with the glass transition (dynamic glass transition), are critically discussed.

Experimental Part

Details of the preparation and characterization of the materials have been given elsewhere.[14–17] The nanocomposites investigated include: (1) epoxy resin/modified smectite clay (ER/clay) nanocomposites of exfoliated structure[14]; (2) epoxy resin/nanosized carbon particle (ER/NCP) nanocomposites with a mean particle diameter of about 10 nm[15]; (3) epoxy resin/diamond (ER/diamond) nanocomposites with a mean particle diameter of about 6 nm[16]; (4) styrene-butadiene rubber/silica (SBR/silica) nanocomposites[6]; (5) polyimide-silica (PI/silica) nanocomposites prepared by sol-gel techniques.[17]

For ac dielectric spectroscopy measurements the complex dielectric function, $\varepsilon = \varepsilon' - i\varepsilon''$, was determined as a function of frequency and temperature.[12,13] In addition to ac dielectric spectroscopy measurements, the non-isothermal dielectric technique of thermally stimulated depolarization currents (TSDC) was used. TSDC consists of measuring the thermally activated release of frozen-in polarization and corresponds to measuring dielectric losses as a function of temperature at low equivalent frequencies of 10^{-2}–10^{-4} Hz.[18] Details of the measurements and of the various formalisms used for the presentation and analysis of the data have been given elsewhere.[14–17]

Results and Discussion

Overall Dielectric Behavior

Figure 1 shows results obtained with SBR/silica nanocomposites.[6] The composition

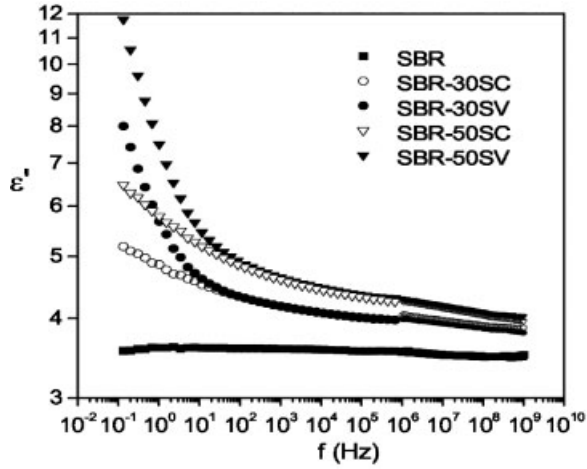

Figure 1.
Real part of dielectric function ε' against frequency f at 25 °C for the SBR/silica nanocomposites indicated on the plot.

of SBR was 23.5 wt% styrene and 76.5 wt% butadiene. The filler used (30 and 50 wt%, nominal) was a precipitated amorphous silica, non-treated (code SV) and pre-treated (code SC) to render the surface organophilic.[6] The results show that ε' increases with increasing amount of filler. This can be understood in terms of a higher dielectric constant of the filler than the matrix and effective medium formulae[17] and/or increased molecular mobility of the polymeric chains. The values of ε' in the nanocomposites of Figure 1 exceed, however, those of pure silica ($\varepsilon' = 3.8$–4.0 at 25 °C[17]), indicating that the data can not be explained solely on the basis of mixture formulae. The hypothesis of increased molecular mobility of the polymeric chains resulting from increase of free volume due to loosened molecular packing of the chains confined between the nanoparticles[19] will be further discussed later on the basis of results for the dielectric strength (magnitude) of secondary and primary relaxations.

A dielectric relaxation is observed in Figure 1 (step in $\varepsilon'(f)$) centered at 10^6–10^7 Hz. This is the segmental α relaxation associated with the glass transition of SBR to be studied in more detail in the next section. The increase in $\varepsilon'(f)$ with decreasing frequency for $f \leq 10^3$ Hz, not observed in the pure matrix, originates from space charge polarization and dc conductivity effects. The results in Figure 1 show that these effects are more pronounced in the samples with non-treated silica particles, whereas dipolar effects at higher frequencies do not depend on filler treatment. It is reasonable to assume that space charge polarization originates from the accumulation of charges in the volume of polymer trapped within agglomerates formed by the nanoparticles. The higher values of space charge polarization in the composites with non-treated filler suggest then that the degree of agglomeration is larger in these composites. These results suggest that low-frequency ac measurements are sensitive to changes in the morphology, in agreement with results for the glass transition and the α relaxation by DRS and DSC (this work) and by DMA.[6]

Figure 2 shows TSDC and Figure 3 ac results for the ER/NCP nanocomposites. The data in Figure 3 have been recorded isothermally by scanning the frequency and have been replotted here. A relatively high frequency has been chosen for the presentation, in order to eliminate conductivity effects present at lower frequencies. An

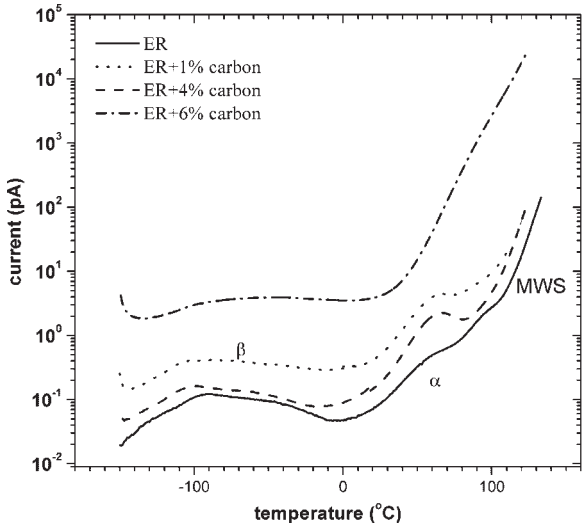

Figure 2.
TSDC thermograms for the ER/carbon nanocomposites indicated on the plot.

overall increase of molecular mobility is observed in Figure 3, in agreement with TSDC data for the same samples shown in Figure 2, in the sense that, at each temperature, ε' and ε'' increase with increasing filler content. This is to a large extent related to the formation of a percolation structure of the nanoparticles, as confirmed by the dependence of ε' (at a frequency of 1Hz and a temperature of $-50\,^{\circ}C$) on volume concentration p of NCP in the inset to Figure 3(a). The well-known equation for the dependence of ε' on p from percolation theory.[20]

$$\varepsilon'(p) = \varepsilon'_m + A|p - p_c|^{-t} \quad (1)$$

where m refers to the matrix, p_c is the percolation threshold and t the critical exponent, has been fitted to the data and the values of p_c and t determined to 7.4% and 0.69 respectively. Two relaxations, a secondary β relaxation at lower temperatures and the segmental α relaxation at

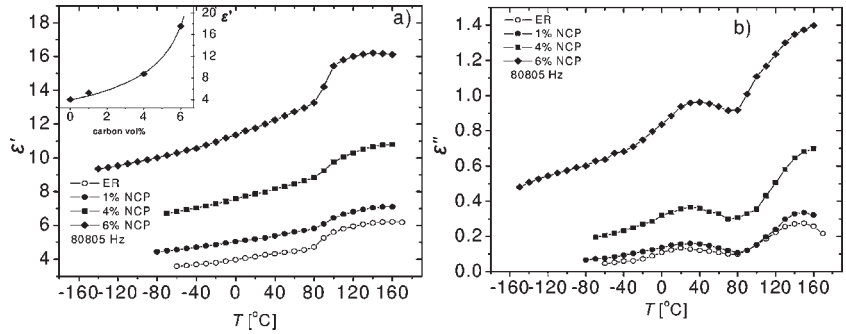

Figure 3.
Temperature dependence of the real ε' (a) and the imaginary part ε'' (b) of the dielectric function of the samples indicated on the plot at 80805 Hz. The inset shows ε' (measured at 1Hz and $-50\,^{\circ}C$) against volume concentration of NCP. The line is a fit of Equation (1) to the data.

higher temperatures, associated with the glass transition of the ER matrix, are observed in Figure 3. They will be studied in more detail in following sections. In the TSDC measurements on the same samples in Figure 2, in addition to the β and the α relaxations, an interfacial Maxwell-Wagner-Sillars (MWS) relaxation is observed in the ER matrix at higher temperatures (interestingly, however, not in the nanocomposites).

Figure 4 shows results obtained with PI/silica nanocomposites prepared by the in situ generation of crosslinked organosilicon nanophase through the sol-gel process.[17] The step at higher frequencies is due to the secondary γ relaxation of the PI matrix, to be discussed in the next section. The most interesting result in Figure 4 is the overall and monotonous decrease of ε' with increasing filler content. Moreover, the values are lower than those of bulk silica ($\varepsilon' = 3.8$–4.0), suggesting a looser molecular packing of PI chain fragments adjacent to the filler particles and/or a loose inner structure of the spatial aggregates of the organosilicon nanophase. By assuming a constant value of ε' for the PI matrix (the measured one, $\varepsilon'_m = 3.18$) and by using various effective medium theory formulae for the calculation of the dielectric function of a composite material[17,20] we obtained for the organosilicon nanophase ε'_i values between 2.47 and 1.58, depending on the composition and the specific formula used. The ε'_i values show, however, the same trend with composition, independently of the formula used. These results can be rationalized assuming that the organosilicon nanophase is made up of nanoparticles of silica ($\varepsilon'_m = 3.8$–4.0) fused together into loose spatial aggregates with a considerable fraction of empty inner pockets ($\varepsilon'_i = 1$). Effective medium theory calculations for this silica-air composite give for the volume fraction of air values in the range 0.40–0.65.[17]

Secondary Relaxations

The step in ε'(f) in Figure 4 at frequencies higher than about 10^4 Hz is due to the local γ relaxation of the PI matrix, tentatively attributed to non-cooperative motions of the imide groups and/or adsorbed water.[17] Figure 5 shows results for the same γ relaxation in another series of PI/silica nanocomposites, prepared also by sol-gel techniques.[19] The magnitude of the relaxation increases with increasing silica content, without any change of the time scale. Similar results were obtained by TSDC measurements (also in the PI/silica nanocomposites of Fig. 4). Measurements on the same PI/silica samples at different water contents by ac

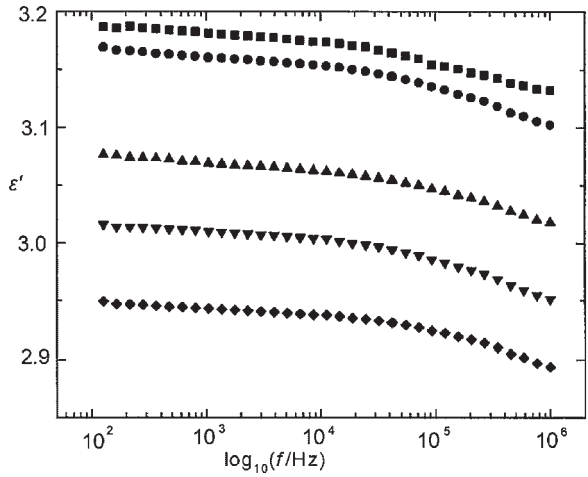

Figure 4.
Frequency dependence of the real part of the dielectric function ε' at 25 °C for PI/silica nanocomposites. The weight fraction of silica is from the uppermost to the lowermost curve 0, 8.6, 22.4, 31.7, 35.6.

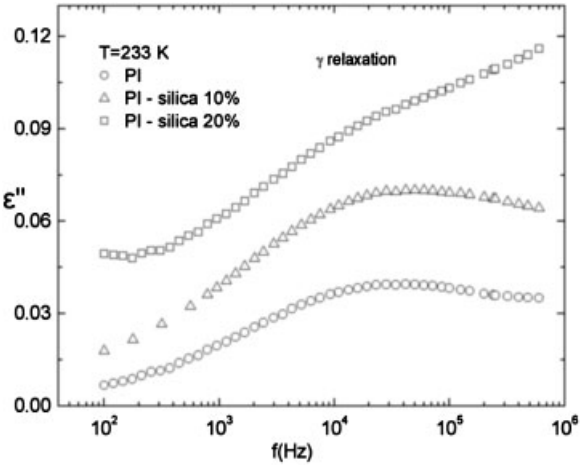

Figure 5.
Frequency dependence of dielectric losses ε'' of the PI/silica nanocomposites indicated on the plot in the region of the γ relaxation.

dielectric spectroscopy and by TSDC indicate that adsorption of water has the same effect on the γ relaxation as the increase of silica content. The effects of water in PIs are commonly explained in terms of plasticization and increase of free volume.[19] Thus, our results suggest that the same explanation may apply for the effects of silica inclusions on the local-scale dynamics in PIs.

Analysis of the various relaxation mechanisms in the nanocomposites under investigation was done by fitting an appropriate model function to the experimental data, typically the Havriliak-Negami (HN) function,[12,13] and analysis in terms of time scale, relaxation strength and shape of the response. Analysis of the data for the γ relaxation of the PI/silica nanocomposites of Figure 4 in terms of the time scale (loss peak frequency f_{max}) shows that the relaxation becomes faster in the nanocomposites. The Arrhenius equation [12,13]

$$f_{\max} = f_0 \exp(-E_{\text{act}}/kT) \qquad (2)$$

where E_{act} is the apparent activation energy, f_0 the pre-exponential frequency factor and k Boltzmann's constant, was fitted to the data for the temperature dependence of f_{max} (Arrhenius plot) and E_{act} and f_0 determined for each composition. Both E_{act} and f_0 tended to decrease with increasing filler content, from $E_{act} = 49$ kJ/mol and $logf_0 = 14.1$ in pure PI to $E_{act} = 36$ kJ/mol and $logf_0 = 12.2$ in the composite with 35.6 wt-% organosilicon nanophase. These results are in agreement with the hypothesis of increased free volume in the nanocomposites due to loosened molecular packing of the chains close to the nanoparticles. Calculations have indicated a decrease of polymer density around a sphere, in particular for short chains.[21] Measurements have shown that the self-diffusion constant of pentane in a polymer characterized by high permeability increases on addition of nanoparticles, and this result has been explained in terms of increased free volume.[22]

We discuss now the results for the β relaxation of ER in the ER/NCP nanocomposites of Figures 2 and 3. The β relaxation in ER has been associated with motions of the hydroxypropylether group.[23] The magnitude of the relaxation increases in the nanocomposites, whereas the time scale (temperature position) of the response does not change appreciably with the composition, similarly to the results for the PI/silica nanocomposites of Figure 4. The Arrhenius plot provides more details on the dynamics of the β relaxation. Similarly to the results in

PI/silica nanocomposites, the apparent activation energy in the Arrhenius Equation (2) decreases in the nanocomposites (69 kJ/mol in ER, 51, 59, 63 kJ/mol in the nanocomposites with 1, 4, 6% NCP respectively), as does the corresponding frequency factor.

Segmental α Relaxation and Glass Transition

Figure 6 refers to the SBR/silica nanocomposites of Figure 1 and shows isochronal $\varepsilon''(T)$ plots in the region of the primary α relaxation associated with the glass transition. For SBR and SBR-30SC a HN expression was fitted to the data following an evaluation method proposed by Schoenhals and coworkers.[23] The results in Figure 6 suggest that the relaxation shifts slightly to lower temperatures in the nanocomposites, whereas they are less conclusive with respect to the magnitude of the relaxation. Analysis by HN fittings suggests no significant broadening of the response in the nanocomposites. DSC measurements on the same samples show, in consistency with the dielectric data, that the glass transition temperature T_g decreases slightly, whereas the heat capacity jump ΔC_p at the glass transition decreases more than additivity would predict in the nanocomposites with respect to the pure matrix. The shift of T_g is systematically larger for the pretreated than for the non-treated samples. These results can be understood in terms of two opposite effects[19]: immobilization of a fraction of chains at the interfaces, because of interaction with the particles, which causes a deficit in ΔC_p, and loosened molecular packing of the chains, because of tethering and of geometrical confinement, which leads to increase of free volume and increased chain mobility. Interestingly, the shift of T_g is larger for the pretreated samples, in agreement with a lower degree of aggregation of nanoparticles in these samples, as indicated by the results in Figure 1.

No second glass transition was observed in the SBR/silica nanocomposites, neither by DSC nor by DRS. In poly(dimethylsiloxane)/silica (PDMS/silica) nanocomposites, however, with a fine dispersion of silica nanoparticles of about 10 nm diameter and hydrogen bonding polymer-filler interactions two α relaxations (dynamic glass transitions) were observed by DRS, the slower one corresponding to the polymer in an interfacial layer with a thickness of 2–3 nm around the nanoparticles.[9,24] Interestingly, only a drop of ΔC_p at T_g but no second glass transition were observed in these nanocomposites by DSC.[9]

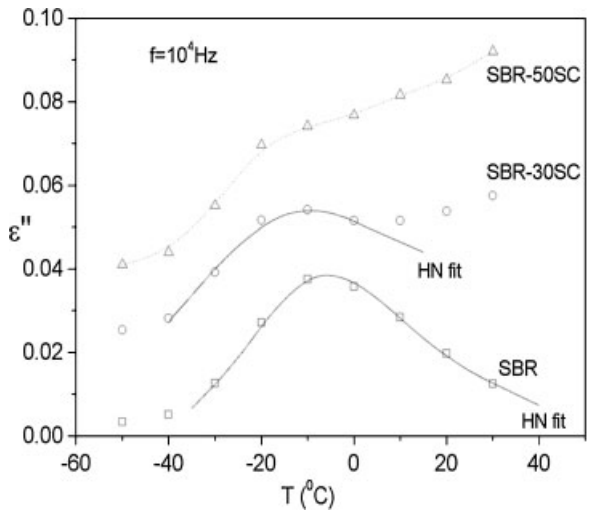

Figure 6.
Isochronal (constant frequency, $f = 10^4$Hz) plot of dielectric loss ε'' against temperature T in the region of the α relaxation for three SBR/silica samples indicated on the plot.

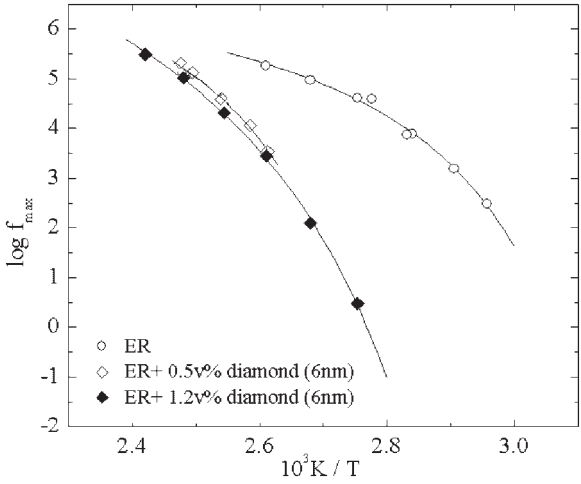

Figure 7.
Arrhenius plot for the α relaxation of the epoxy/diamond nanomposites indicated on the plot. The lines are fits of the VTF Equation (3).

Different results than those in SBR/silica and PDMS/silica, namely a shift of T_g and of the α relaxation to higher temperatures in the nanocomposites as compared to the pure polymer matrix, were obtained for ER/clay[14] and ER/diamond nanocomposites.[16] Despite strong contribution of conductivity and space charge polarization to the measured $\varepsilon'(f)$ and $\varepsilon''(f)$ data in ER/diamond nanocomposites, the dynamics of the α relaxation could be analyzed by calculating, at selected temperatures, $\varepsilon''(f)$ by a derivative method from the measured $\varepsilon'(f)$, where dc conductivity makes no contribution.[25] The frequency of the maximum of the dielectric loss f_{max} for the α relaxation was obtained from the calculated spectra at each temperature and is plotted in the Arrhenius diagram (activation diagram) of Figure 7. The temperature dependence of f_{max} is well described by the Vogel-Tammann-Fulcher (VTF) Equation,[12,13]

$$f_{max} = A \exp[-B/(T - T_0)] \quad (3)$$

where *A, B* and T_0 (Vogel temperature) are temperature independent empirical constants. The α relaxation is significantly slower in the nanocomposites as compared to the matrix; note, however, that doubling the volume fraction of the filler from 0.5% to 1.2% seems to only slightly affect the dynamics.

Conclusions

The results presented above for several nanocomposites indicate that dielectric techniques are very powerful for investigating molecular dynamics in relation to morphology in nanocomposites. Several interesting results were obtained with each of the five systems studied and discussed in relation to results obtained by using other techniques. We would like to stress here two observations, which may apply for more systems. (i) Chemical treatment of the nanoparticles, polymer-filler interactions and details of the method of preparing the nanocomposites are reflected in the characteristics of the cooperative segmental relaxation. (ii) The frequency/temperature position of local relaxations of the polymer matrix is not significantly altered by the presence of the nanoparticles. However, in two of the systems studied (PI/silica and ER/NCP) significant changes of the dynamics were observed, with both the apparent activation energy and the pre-exponential

factor in the Arrhenius equation decreasing significantly in the nanocomposites. Further work is needed to fully understand these changes at the molecular level.

Acknowledgements: The project is co-funded by the European Social Fund (75%) and National Resources (25%) – EPEAEK II – Archimedes II.

[1] M. Alexandre, P. Dubois, *Mater. Sci. Eng.* **2000**, *28*, 1.
[2] S. S. Ray, M. Okamoto, *Prog. Polym. Sci.* **2003**, *28*, 1539.
[3] M. Z. Rong, M. Q. Zhang, Y. X. Zheng, H. M. Zeng, K. Friedrich, *Polymer* **2001**, *42*, 3301.
[4] G. Tsagaropoulos, A. Eisenberg, *Macromolecules* **1995**, *28*, 6067.
[5] J. Berriot, H. Montes, F. Lequeux, D. Long, P. Sotta, *Macromolecules* **2002**, *35*, 9756.
[6] V. Arrighi, I. J. McEwen, H. Qian, M. B. Serrano Prieto, *Polymer* **2003**, *44*, 6259.
[7] F. W. Starr, T. B. Schroeder, S. C. Glotzer, *Macromolecules* **2002**, *35*, 4481.
[8] G. J. Papakonstantopoulos, K. Yoshimoto, M. Doxastakis, P. F. Nealey, J. J. de Pablo, *Phys. Rev. E* **2005**, *72*, 031801.
[9] D. Fragiadakis, P. Pissis, L. Bokobza, *Polymer* **2005**, *46*, 6001.
[10] G. C. Papanicolaou, S. A. Paipetis, P. S. Theocharis, *Colloid Polym. Sci.* **1978**, *7*, 625.
[11] G. C. Papanicolaou, N. K. Anifantis, L. K. Keppas, Th.V. Kosmidou, *Compos. Interf.* **2007**, *14*, 131.
[12] J. P. Runt, J. J. Fitzgerald, Eds, "*Dielectric Spectroscopy of Polymeric Materials*", American Chemical Society, Washington, DC 1997.
[13] F. Kremer, A. Schoenhals, Eds, "*Broadband Dielectric Spectroscopy*", Springer, Berlin 2003.
[14] A. Kanapitsas, P. Pissis, R. Kotsilkova, *J. Non-Cryst. Solids* **2002**, *305*, 204.
[15] R. Kotsilkova, D. Fragiadakis, P. Pissis, *J. Polym. Sci. Part B Polym. Phys* **2005**, *43*, 522.
[16] P. Pissis, D. Fragiadakis, *J. Macromol. Sci. Part B Phys.* **2007**, *46*, 119.
[17] D. Fragiadakis, E. Logakis, P. Pissis, V. Yu. Kramarenko, T. A. Shantalii, I. L. Karpova, K. S. Dragan, E. G. Privalko, A. A. Usenko, V. P. Privalko, *J. Phys. Conf. Ser.* **2005**, *10*, 139.
[18] J. vanTurnhout, " *Thermally Stimulated Discharge of Electrets*", in: "*Electrets. Topics in Applied Physics*", Vol. *33*, G. Sessler, Ed., Springer, Berlin **1980**, pp. 81–215.
[19] V. A. Bershtein, L. M. Egorova, P. N. Yakushev, P. Pissis, P. Sysel, L. Brozova, *J. Polym. Sci. Part B Polym. Phys.* **2002**, *40*, 1056.
[20] R. Pelster, U. Simon, *Colloid Polym. Sci.* **1999**, *277*, 2.
[21] R. Tuinier, H. N. W. Lekkerkerker, *Macromolecules* **2002**, *35*, 3312.
[22] J. Zhong, W. Y. Wen, A. A. Jones, *Macromolecules* **2003**, *36*, 6430.
[23] E. Schlosser, A. Schoenhals, H.-E. Carius, H. Goering, *Macromolecules* **1993**, *26*, 6027.
[24] D. Fragiadakis, P. Pissis, L. Bokobza, *J. Non-Cryst. S. olids* **2006**, *352*, 4969.
[25] J. van Turnhout, M. Wuebbenhorst, *J. Non-Cryst. S. olids* **2002**, *305*, 50.

